



Deep-learning-based porosity monitoring of laser welding process

Bin Zhang, Kyung-Min Hong, Yung C. Shin *

School of Mechanical Engineering, Purdue University, West Lafayette, IN 47907, United States

ARTICLE INFO

Article history:

Received 2 May 2019

Received in revised form 18 December 2019

Accepted 2 January 2020

Available online 3 January 2020

Keywords:

Laser welding

Convolutional neural network (CNN)

Porosity monitoring

ABSTRACT

A porosity monitoring scheme for laser welding process was developed based on a deep learning approach. The in-process weld-pool data were sensed with a coaxial high-speed camera and labelled with the porosity attributes measured from welded specimens. A convolutional neural network (CNN) model with compact architecture was designed to learn weld-pool patterns to predict porosity. In laser welding experiments of 6061 Aluminum alloy, the CNN-based monitoring model achieved a classification accuracy of 96.1% for porosity occurrence detection, though the prediction of micro (less than 100 μm) and deep subsurface pores still remains challenging.

© 2020 Published by Elsevier Ltd on behalf of Society of Manufacturing Engineers (SME).

1. Introduction

The laser welding process, which is featured with high energy density and a small heat affected zone, has become an attractive alternative to the traditional material joining processes [1]. However, the performance of welded parts might be deteriorated by the quality defects that occur during the laser-induced material melting-solidification process, such as porosity, cracking, lack of fusion and incomplete penetration [2], which necessitates a trial-and-error design of the process parameters to minimize defects and expensive post-process metrology for quality inspection. Therefore, to assure the quality consistency of products, a real-time process-level quality monitoring scheme is critically needed for the laser welding processes.

The in-process monitoring of laser welding has been widely investigated [2,3]. Ancona et al. found that the mean and standard deviation of plasma's electron temperature calculated from spectrometer data has a correlation to weld defects like lack of penetration and weld disruptions [4]. Sibillano et al. continued this study and found a quantitative relationship between electron temperature and penetration depth [5]. Bardin et al. measured the keyhole shape and intensity profile to predict lack of penetration in laser welding [6]. Nicolosi et al. described a camera-based full penetration extraction method using cellular neural network [7]. Kim et al. presented a keyhole area estimation method based on coaxial image sensing [8]. You et al. found that with the fusion of photodiode and camera data, it was possible to monitoring the laser-

induced plume and spatters [9] and classify sound and defective weldings [10]. Using the wavelet packet decomposition and principal component analysis for feature extraction, neural networks and support vector machines were then built to detect weld defects like blowouts and undercut, which achieved an accuracy of 81.34% [11]. Luo et al. developed a coaxial camera setup for weld-pool boundary extraction and keyhole size measurement [12], and with the use of a radial basis function network it was possible to predict the keyhole penetration depth and inclination angle. A correlation between porosity and keyhole size was also observed, which revealed that the coaxial images could be potentially used for porosity prediction [13]. Xu et al. have also found that the large fluctuation of keyhole was responsible for the bubble and pore formation [14]. However, an on-line porosity monitoring scheme hasn't been developed in the literature for the laser welding process.

In this paper, a deep-learning-based in-process porosity monitoring scheme was proposed for laser welding. Instead of relying on the artificially defined features like keyhole area, intensity and plasma's electron temperature as in conventional process monitoring studies, a convolutional neural network (CNN) model with automatic feature-learning capacity [15] was designed to extract features from the high dimensional weld-pool image data collected by a high-speed camera. The porosities that occurred during welding were inspected via cross sectioning the welded specimens to label camera images. The CNN model was trained to detect the occurrence of porosity in keyhole laser welding of 6061 Aluminum alloy and achieved a classification accuracy of 96.1%, which proved that the CNN-based monitoring scheme is capable of predicting porosity occurrence accurately.

* Corresponding author.

E-mail address: shin@purdue.edu (Y.C. Shin).

2. Experiment and methodologies

2.1. Instrumentation and experiments

The instrumented laser welding system (a 1000 W fiber laser head mounted on a Mazak CNC machine) in our previous work [12] is used as the testbed for this study, as presented in Fig. 1. The coaxial camera integrated with the laser head is upgraded to a DMK 33UX174 monochrome high-speed camera, which can record 640×480 pixel images at 395 frames per second. The field of view of the camera is about 5.16×3.87 mm, which covers the region of weld pool and its surrounding. The IC Capture software developed by the camera's manufacturer, The Imaging Source, is used to collect image data from the camera during experiments. To alleviate the issue that the high contrast of weld-pool images may exceed the dynamic range of camera, a narrow band pass filter with 532 nm center wavelength is inserted in front of the camera to reduce the impact of weld-pool irradiations, and a 200 mW green laser is used to illuminate the weld-pool surrounding.

A set of lap laser welding experiments were conducted using AA6061 Aluminum alloy plates. The plate thickness was 1 mm and the interface gap between two plates was controlled to be zero, since eliminating the gap tends to yield the maximum porosity [16] and facilitate the building of data-driven porosity monitoring model, given that more data samples with porosity could be collected. The welding speed was chosen as 1400 mm/min and the laser power was 1000 W, which would give the best quality in terms of surface appearance as suggested by [16]. With the selected welding speed, the space resolution of camera images was about $59 \mu\text{m}/\text{frame}$. The length of each weld track depends on the length of plates and is summarized in Table 1.

2.2. Porosity measurement

To label the collected weld-pool images with the quality attributes to be predicted, the porosity in welded specimens was inspected via cross sectioning the specimens along the laser scan direction at the center of each track, given that porosity is most likely to occur at the center of weld pool. The cross-sectioning method is more affordable than the non-destructive X-ray tomography method and is efficient to capture most of the large pores around the center of weld pore. An optical microscope was used to observe the pores exposed on the cross section and a set of image processing tools were developed in MATLAB to extract porosity attributes from microscope images [17]: 1) consecutive cross-section images were concatenated via the matching of SURF (speeded-up-robust-features) points [18]; 2) then the concatenate

Table 1

Experimental conditions in laser welding.

Test#	Speed (mm/min)	Power (W)	Length (mm)
1	1400	1000	47.6
2	1400	1000	65.7
3	1400	1000	75.2

ated image was binarized with a Qtsu's threshold and the dark regions with an extent (ratio of number of pixels in the region to the number of pixels in its bounding box) larger than 0.3 and eccentricity less than 0.9 were recognized as true pore regions; 3) the porosity attributes like porosity status (true: pore, false: no pore) and size were extracted from each porosity region and paired with the weld-pool images at corresponding longitudinal positions to form an input–output data pair that can be used to train the supervised deep learning model. The image processing procedure is illustrated in Fig. 2. The extent and eccentricity thresholds were applied when identifying porosity because there're two types of pores observed: 1) circular pores inside the upper plate caused by entrapped gas, which were the targets for porosity detection and 2) irregular pores caused by material cracking or tearing at the weakly bonded plate interface, which might be introduced when preparing the cross section and should be excluded from data labeling. Examples of rejected and accepted candidate pores are given in the part 2 of Fig. 2.

2.3. Convolutional neural network

A convolutional neural network (CNN) model, which transforms the weld-pool images into compressed internal representations through discrete convolution of the raw images with a set of automatically-tuned filters, is designed to learn weld-pool patterns to predict the porosity attributes. Due to its automatic pattern learning capacity from raw image data, the CNN model could establish the feature extractor and classifier conjunctively in its training routine and hence doesn't require the tedious engineering of features from raw data as in conventional machine learning models like support vector machine. The architecture of the CNN model designed in this work is shown in Table 2, which is similar to the benchmark AlexNet [19]. However, the number of layers and number of filters in each of the convolutional layers was reduced until a noticeable drop of performance was observed. The number of learnable parameters was substantially reduced through the architecture reduction so that the model can be trained with smaller data sets. Between the convolutional layers, batch normalization was used to allow a higher learning rate [20], max pooling was used to down-sample the feature maps and rectified linear unit (ReLU) was used to introduce nonlinearity. Two fully connected layers after the last convolutional layer were used as the classifier to predict porosity based on the features extracted from convolution. A backpropagation algorithm with stochastic gradient searching called Adam [21] was adopted to train the network.

3. Results and discussion

After labeling the coaxial weld-pool images with porosity status measured from corresponding longitudinal positions, the CNN model was built by using Test#1 and #2 for training (1971 samples) and Test#3 for validation (1276 samples). The trained model achieved a classification accuracy of 97.8% on the training data set and 96.1% on the validation data set. The predictions of the CNN model was compared with cross-section measurement in Fig. 3 for one of the training set Test#1 and in Fig. 4 for the validation set Test#3. It can be seen that though the CNN model correctly

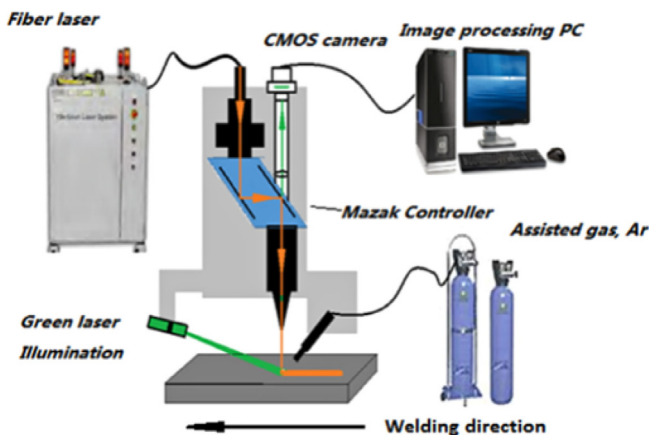


Fig. 1. Diagram of the coaxial monitoring system [12].

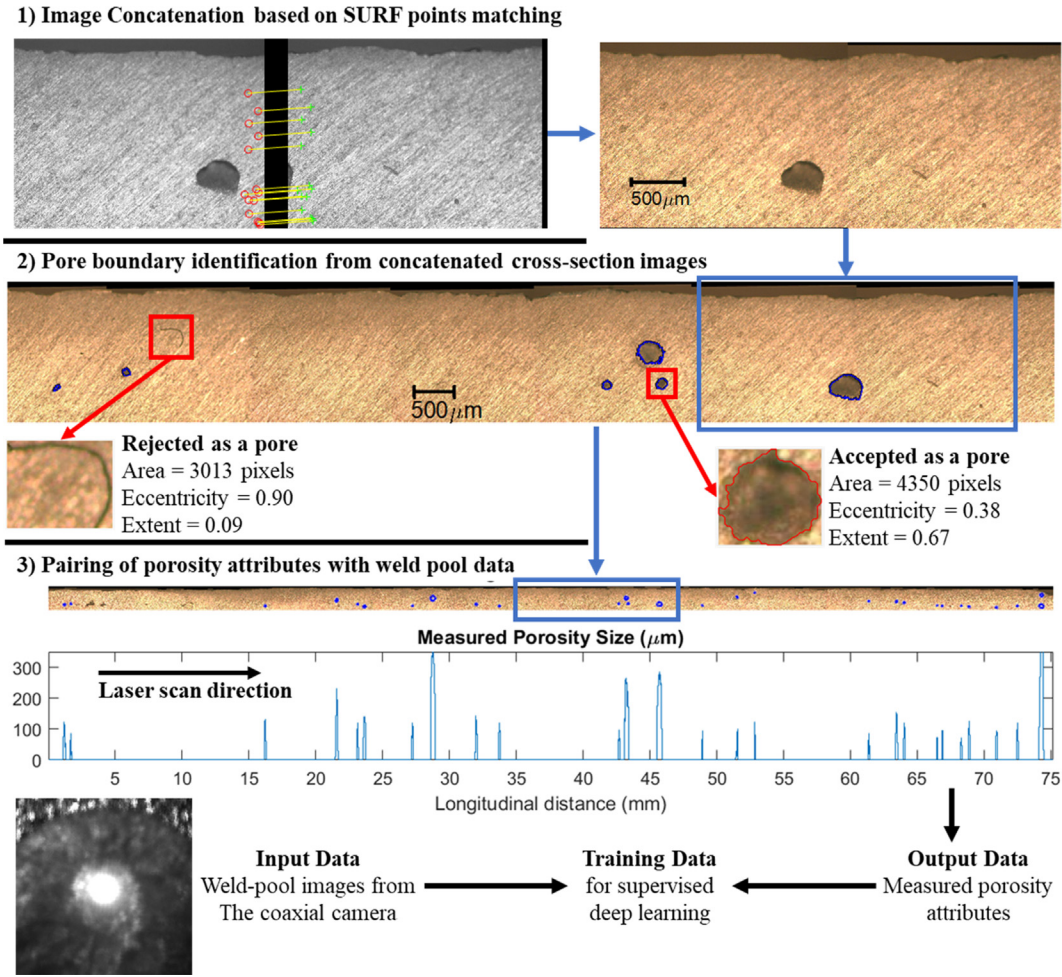


Fig. 2. Illustration of image processing and training data preparation.

Table 2
Architecture of the convolutional neural network.

Layer	Filter Size	Number of filters	Stride	Max Pooling
Image Input	224 × 224 grayscale images			
Convolution	11	96	4	8 × 8, stride of 2
Convolution	5	96	2	4 × 4, stride of 2
Convolution	3	128	1	3 × 3, stride of 2
Convolution	3	192	1	3 × 3, stride of 2
Fully Connected	32 output channels			
Fully Connected	2 output for classification			

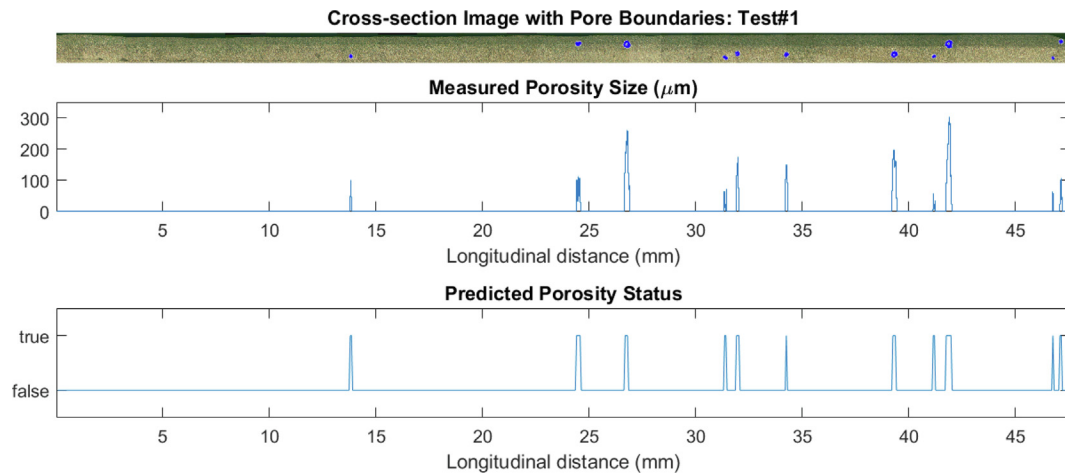


Fig. 3. Porosity occurrence detection for laser welding: training set Test#1.

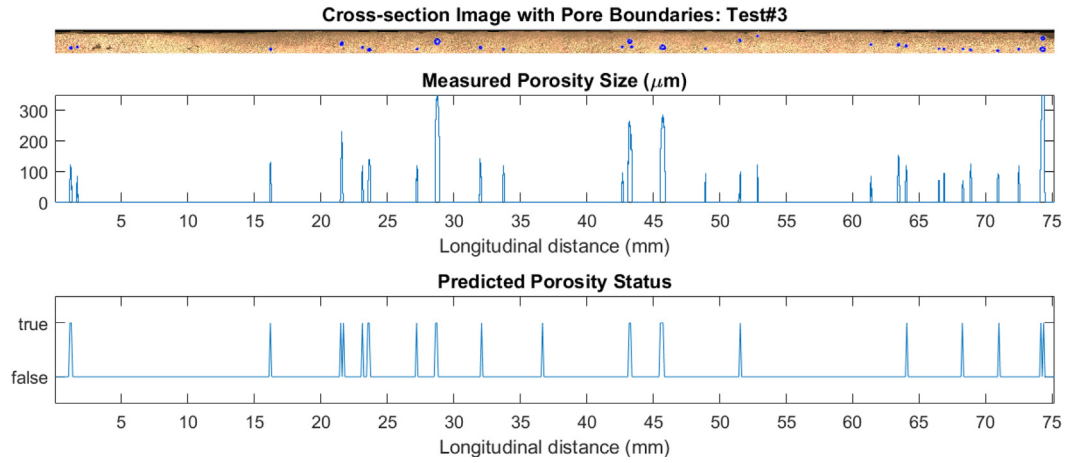


Fig. 4. Porosity occurrence detection for laser welding: validation set Test#3. Top: the cross section image with extracted pore boundaries highlighted; Middle: pore size measured from the cross section; Bottom: CNN classification results.

detected all the pores in the training set, it failed to capture some pores in the validation set. By looking into those misclassified pores, it was found that they're mainly the pores of small or medium size (below or around 100 μm) and were mostly distributed

close to the interface of two overlapping plates. Owing to their limited size and deep location, these pores might be not able to produce sufficient impact on the melt pool to make themselves detectable.

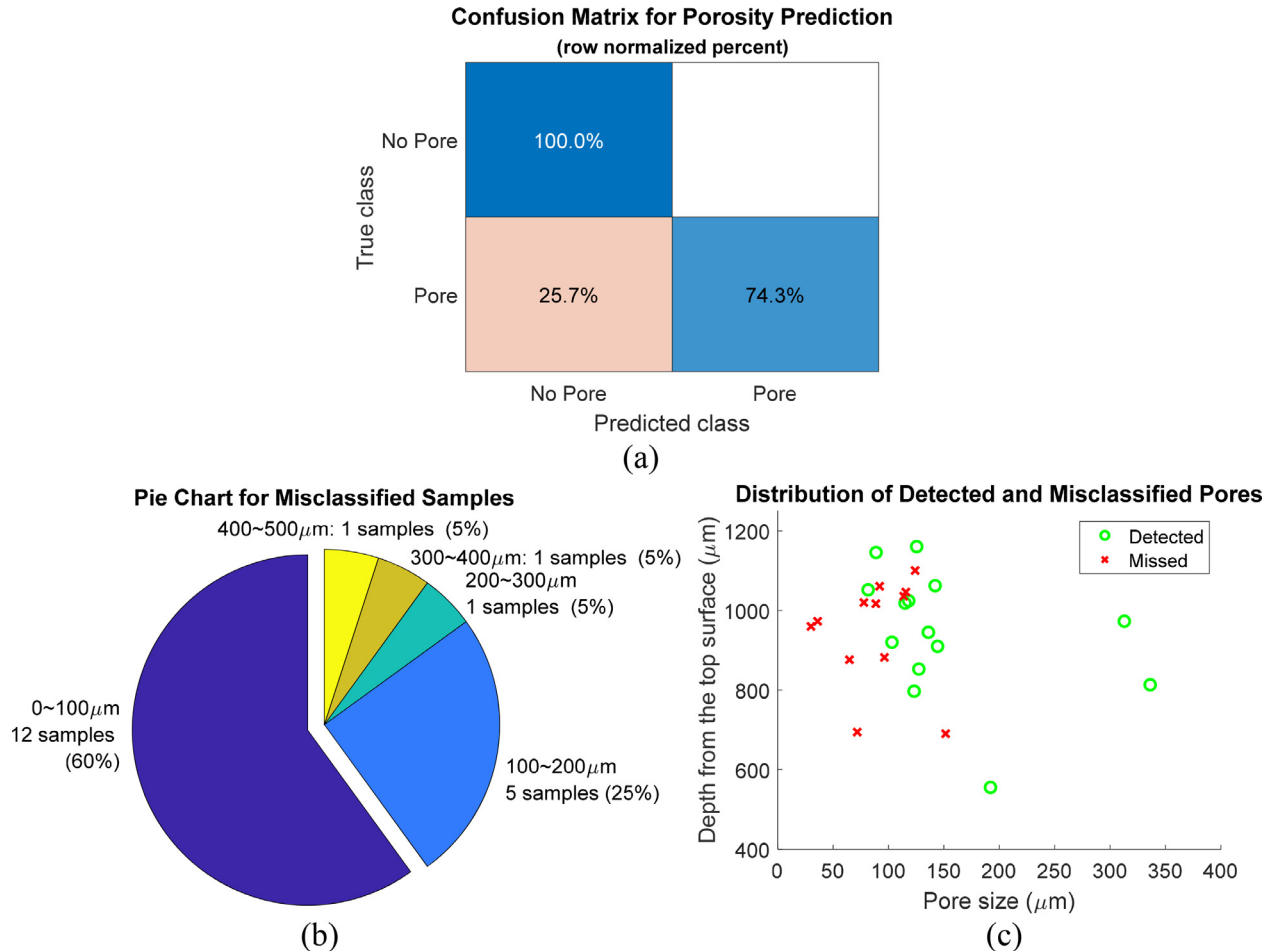


Fig. 5. Statistics of the CNN porosity status prediction for laser welding. (a) Confusion matrix showing the percent of correctly and incorrectly classified samples (b) Pie chart showing the distribution of misclassified samples in validation set; (c) Distribution of the size and depth of detected and misclassified pores in validation set.

As described in Section 2.2, extent and eccentricity thresholds were applied to select only the true gas pores and reject irregular cracks and scratches. For example, the large irregular cavities at the longitudinal position of about 3–5 mm in Test#3 (see top plot of Fig. 4), which were located close to the interface, were not labeled as pores. However, for the small pores close to the interface and with near-circular shapes, it was difficult to set appropriate criteria to classify them into one of the two distinct types and hence caused mislabeling of data. The statistics in Fig. 5 verifies that failing to detect those small ($<150\text{ }\mu\text{m}$) and deep ($>800\text{ }\mu\text{m}$ below top surface and close to interface) pores were the primary source of classification error, because all the misclassified samples are false negative samples (Fig. 5a) with small size (Fig. 5b) and deep location (Fig. 5c). Overall, the CNN model trained for laser welding exhibited sufficient fidelity in detecting the large pores above $100\text{--}150\text{ }\mu\text{m}$, which were more fatal to the strength of material joining than those small pores the model failed to detect.

4. Conclusions

The in-process porosity monitoring of laser welding process was studied in this paper using deep-learning approach. A convolutional neural network (CNN) were designed to predict porosity based on the coaxial weld-pool data sensed by a high-speed camera. Experimental results show that the CNN model could detect the porosity occurrence with an accuracy of 96.1% in lap laser welding of 6061 Aluminum alloy. It was also found that for a pore to be detectable, it must produce sufficient impact on the weld pool that can be captured by the camera. This explains why the prediction error in this paper is mainly caused by the small (less than $150\text{ }\mu\text{m}$) and deep (close to interface) pores. Upgrading the coaxial camera to higher resolution and frame rate to better sense small pores and extending the predictive model to larger data sets and wider range of operating conditions will be the future effort to be made to develop a porosity monitoring scheme that can be implemented on industrial-level laser welding systems.

Declaration of Competing Interest

The authors declare that they have no known competing financial interests or personal relationships that could have appeared to influence the work reported in this paper.

References

- [1] Hong KM, Shin YC. Prospects of laser welding technology in the automotive industry: a review. *J Mater Process Technol* 2017;245:46–69.
- [2] Stavridis J, Papacharalampopoulos A, Stavropoulos P. Quality assessment in laser welding: a critical review. *Int J Adv Manuf Technol* 2018;94(5–8):1825–47.
- [3] You DY, Gao XD, Katayama S. Review of laser welding monitoring. *Sci Technol Weld Join* 2014;19(3):181–201.
- [4] Ancona A, Spagnolo V, Lugara PM, Ferrara M. Optical sensor for real-time monitoring of CO₂ laser welding process. *Appl Opt* 2001;40(33):6019–25.
- [5] Sibillano T, Rizzi D, Ancona A, Saludes-Rodil S, Nieto JR, Chmélíčková H, et al. Spectroscopic monitoring of penetration depth in CO₂ Nd: YAG and fiber laser welding processes. *J Mater Process Technol* 2012;212(4):910–6.
- [6] Bardin F, Cobo A, Lopez-Higuera JM, Collin O, Aubry P, Dubois T, et al., 2005. Optical techniques for real-
- [7] Nicolosi L, Tetzlaff R, Abt F, Blug A, Carl D, Hofler H. New CNN based algorithms for the full penetration hole extraction in laser welding processes: experimental results. In: 2009 international joint conference on neural networks. IEEE; 2009. p. 2256–63.
- [8] Kim CH, Ahn DC. Coaxial monitoring of keyhole during Yb: YAG laser welding. *Opt Laser Technol* 2012;44(6):1874–80.
- [9] You D, Gao X, Katayama S. Monitoring of high-power laser welding using high-speed photographing and image processing. *Mech Syst Sig Process* 2014;49(1–2):39–52.
- [10] You D, Gao X, Katayama S. Multisensor fusion system for monitoring high-power disk laser welding using support vector machine. *IEEE Trans Ind Inf* 2014;10(2):1285–95.
- [11] You D, Gao X, Katayama S. WPD-PCA-based laser welding process monitoring and defects diagnosis by using FNN and SVM. *IEEE Trans Ind Electron* 2015;62(1):628–36.
- [12] Luo M, Shin YC. Vision-based weld pool boundary extraction and width measurement during keyhole fiber laser welding. *Opt Lasers Eng* 2015;64:59–70.
- [13] Luo M, Shin YC. Estimation of keyhole geometry and prediction of welding defects during laser welding based on a vision system and a radial basis function neural network. *Int J Adv Manuf Technol* 2015;81(1–4):263–76.
- [14] Xu J, Rong Y, Huang Y, Wang P, Wang C. Keyhole-induced porosity formation during laser welding. *J Mater Process Technol* 2018;252:720–7.
- [15] Gu J, Wang Z, Kuen J, Ma L, Shahroudy A, Shuai B, et al. Recent advances in convolutional neural networks. *Pattern Recogn* 2018;77:354–77.
- [16] Pellone L, Inamke G, Hong KM, Shin YC. Effects of interface gap and shielding gas on the quality of alloy AA6061 fiber laser lap weldings. *J Mater Process Technol* 2019.
- [17] Zhang B, Liu S, Shin YC. In-Process monitoring of porosity during laser additive manufacturing process. *Addit Manuf* 2019;28:497–505.
- [18] Bay H, Ess A, Tuytelaars T, Van Gool L. Speeded-up robust features (SURF). *Comput Vis Image Underst* 2008;110(3):346–59.
- [19] Krizhevsky A, Sutskever I, Hinton GE. Imagenet classification with deep convolutional neural networks. In: Advances in neural information processing systems. p. 1097–105.
- [20] Ioffe, S. and Szegedy, C., 2015. Batch normalization: Accelerating deep network training by reducing internal covariate shift. arXiv preprint arXiv:1502.03167.
- [21] Kingma, D.P. and Ba, J., 2014. Adam: A method for stochastic optimization. arXiv preprint arXiv:1412.6980.